Stress and Morphology Evolution during Island Growth

Chun-Wei Pao and David J. Srolovitz

Department of Mechanical and Aerospace Engineering, Princeton University, Princeton, New Jersey 08544, USA
Princeton Institute for the Science and Technology of Materials, Princeton University, Princeton, New Jersey 08544, USA

(Received 30 December 2005; published 11 May 2006)

We performed a series of hybrid molecular-dynamics simulations of island growth on a substrate and monitored island stress evolution for several different island/substrate interfacial energies. Smaller (larger) interfacial energy yields islands with a stronger (weaker) compressive stress-thickness product. We present analytical results that suggest that the stress-thickness product is a linear function of the substrate coverage, with slope equal to minus the substrate surface stress, if the island is in mechanical equilibrium, and verify these results with simulation data.

DOI: 10.1103/PhysRevLett.96.186103 PACS numbers: 81.15.Aa, 68.60.Bs, 81.10.Aj, 81.10.Bk

The evolution of the stresses within a film during vapor deposition is complex. In cases where the film evolves via island nucleation and growth to coalescence to produce a continuous polycrystalline nonepitaxial film [Volmer-Weber (VW) growth], the film stresses generated can be very large, the sign of the stress can change rapidly, and interrupting the deposition causes large, abrupt changes in the stress [1,2]. Wafer curvature measurements [3] show that evolution of film stress during VW growth in many different systems shares a common set of characteristics [2,4,5]: The film stress is compressive during island nucleation and growth, then becomes tensile as the growing islands impinge on one another, and then slowly becomes increasingly compressive as the continuous film thickens. (In some cases, the different regimes are not well-separated—see, e.g., Ag on SiO_2 [2].) While the tensile rise upon island impingement is relatively well understood [6,7] and several models have been proposed for the stress evolution mechanism that occurs on film thickening [1,8], the origin of the compressive stress observed during the island growth stage remains poorly understand. Earlier models for this compressive film stress were based on capillarity-induced stress in the islands constrained by the substrate during growth [9,10] or upon the effects of surface defects on surface stresses [11–13]. In the present study, we employ a hybrid static-relaxation–molecular-dynamics (MD) simulation method to determine the origin of the large compressive stresses inside islands that develop prior to island coalescence and propose a theoretical model for this effect that accurately reproduces both simulation and experimental results.

Island growth is characterized by both the deposition of atoms from the vapor and surface diffusion controlled transport of atoms along the surface. However, typical MD simulations do not explore times sufficient to observe many diffusion hops at typical film growth temperatures. In the present study, we combine static-relaxation and finite temperature MD simulations to model the growth of well-separated islands. The island growth algorithm is as follows: First, we release a test atom from many different initial atom positions above the substrate and find its equilibrium position by minimizing the energy of the system using a conjugate gradient method while all other atom positions remain fixed. This is repeated for initial atom positions located on a square grid above the substrate (nearest neighbor spacing equal to the first neighbor spacing in the island). Then we deposit an adatom at the location corresponding to the test atom with the lowest relaxed energy (compared to all of the other test atoms released from the grid). Next we perform a 10 ps MD simulation on the entire system. This process is repeated until the appropriate number of atoms is deposited (deposition is terminated before islands interact across the periodic boundary conditions).

The island geometry is shown in Fig. 1. Although only a single layer of atoms in the substrate is shown in the (111) oriented substrate, the substrate is actually 34 Å thick (14 atomic planes) and is 57.16×57 Å^2 in the X and Y directions, respectively [i.e., 418 atoms/(111) plane]. The MD simulations were performed at a constant temperature $T = 300$ K, and the dimensions of the unit cell in the directions parallel to the substrate surface were fixed. We describe the atomic interactions using a simple parametrized potential appropriate for metallic alloys, that is, the Lennard-Jones embedded-atom method (LJ-EAM) potential [14,15]. The substrate is composed entirely of A atoms and the film or island of B atoms. This potential has the following form: $E = \sum_i [F_{t_i}(\bar{\rho}_i) + \frac{1}{2}\sum_{j \neq i} \phi_{t_i t_j}(r_{ij})]$, where the subscript t_i denotes the element type ($=A$ or B) of atom i, $F_{t_i}(\bar{\rho}_i)$ is the energy required to embed atom i in an electron gas of density $\bar{\rho}_i$, and $\phi_{t_i t_j}(r_{ij})$ denotes the pairwise interaction between atoms i and j [16]. The functional forms of F, $\bar{\rho}$, and ϕ are as described in Ref. [15]. The potential parameters, summarized in Table I, were chosen such that pure A and pure B are both face centered cubic, and the 300 K lattice parameter of pure B is 1.3 times larger than that for pure A in order to avoid epitaxy between the islands and substrate [14].

Since experimental evidence suggests the interfacial bond strength affects the stress evolution during film growth [2], we treat $\varepsilon_{t_i t_j}$ in the pairwise term in the energy

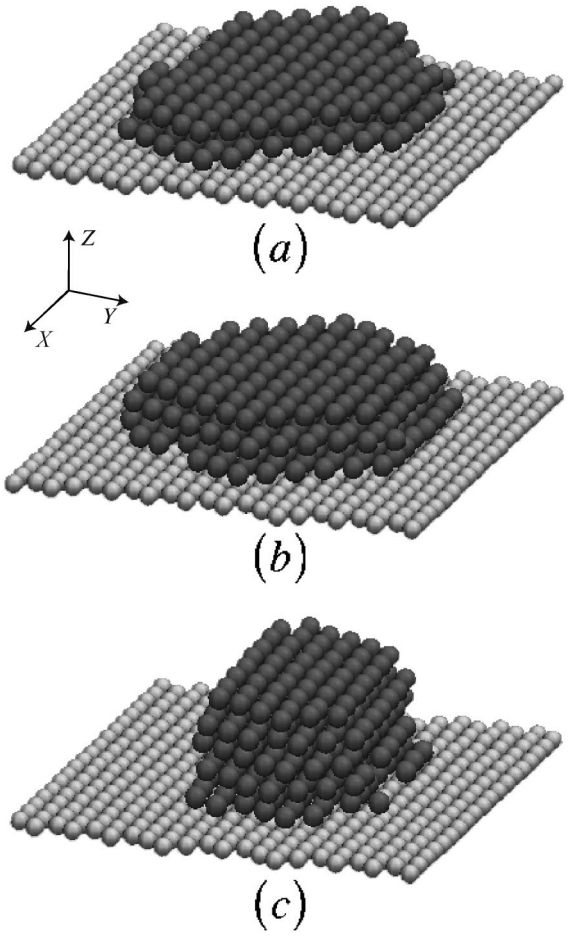

FIG. 1. The morphologies of islands grown with (a) strong, (b) intermediate, and (c) weak interfacial bonding. Dark and light gray atoms represent island and substrate atoms, respectively.

$\phi_{t_i t_j}(r_{ij})$ as an adjustable parameter for $t_i \neq t_j$. Table II shows the (111) surface energies (γ_A and γ_B) and surface stresses (f_A and f_B) [17] of materials A and B, along with the A-B interfacial energy $\gamma_{A\text{-}B}^{(111)}$ for three different values of ε_{AB} (i.e., different interfacial bond strengths): 0.50 (weak), 0.53 (intermediate), and 0.55 eV (strong). Using the Young-Dupre relation, we can relate the surface or interface energies to the equilibrium wetting angle θ. For the range of ε_{AB}, the wetting angle varies from 0° (complete wetting) to 68° (partial wetting).

TABLE I. Parameters used in the LJ-EAM interatomic interactions (following the notation of Ref. [15]).

Pair	$\varepsilon_{t_i t_j}$ (eV)	$r^0_{t_i t_j}$ (Å)	A_t	β_t	Z_0
A-A	0.8	3	0.8	6	12
B-B	0.5	3.9	0.8	6	12
A-B (strong)	0.55	3.6	···	···	···
A-B (intermediate)	0.53	3.6	···	···	···
A-B (weak)	0.5	3.6	···	···	···

Figure 1 shows the structure of typical islands grown with different interfacial bond strengths. The islands formed were all face centered cubic [this is ambiguous for the island in Fig. 1(a) since the island is only two layers thick] with the [111] direction perpendicular to the substrate. In all cases, the interface contains a regular, triangular array of misfit dislocations with four close packed rows of atoms in the substrate for every three close packed rows of atoms in the islands. This implies that the misfit strain is nearly fully relaxed, since B atoms are 1.3 times larger than A. Comparison of the shapes of the islands formed with different A-B bond strength (see Fig. 1) shows that, as the A-B bond strength increases (A-B interface energy decreases), the islands become thinner, with a broader island/substrate contact (i.e., larger radius-to-height aspect ratio). If we assume the surface energy of the island is isotropic, the equilibrated island shape will be a section of a sphere, and the island height h will be a function of its volume V and wetting angle θ: $h = (1 - \cos\theta)(V/\pi)^{1/3}[(2/3) - \cos\theta + (1/3)\cos^3\theta]^{-1/3}$. Table II shows the predicted island height from this expression and the island height measured from the simulations (Fig. 1). The predicted and actual island heights are in good qualitative (semiquantitative) agreement: In each case, the predicted and actual island heights do not differ by more than one atomic layer thickness. Therefore, we can understand the variation of island shape with A-B bond strength directly in terms of its effect on interfacial energy. This result also demonstrates that the hybrid simulation method produces nearly equilibrated islands.

To determine the stress-thickness product (this is proportional to substrate wafer curvature normally used as a measure of film stress in experiment), we imagine cutting our model system along a plane that is orthogonal to the substrate surface and calculate the difference in the normal force across the cut plane before and after island deposition. The stress-thickness product is $\sigma_{xx}h = (F_x - F_x^0)/L_y$ for the X direction, with h the average thickness of the film (whether a continuous film or an array of islands), L_y is the cell length along the Y direction, and F_x and F_x^0 are the normal forces in the X direction after or before the island is

TABLE II. Substrate (A) and island (B) {111} surface energies γ and surface stress f, substrate/island interface energies for different A-B bond strengths (J/m^2), the predicted isotropic equilibrium wetting angle θ, and the predicted and measured (from Fig. 1) island heights h (in units of the number of {111} layers).

	A(111)	B(111)	A-B (strong)	A-B (intermediate)	A-B (weak)
γ	1.58	0.58	0.95	1.12	1.36
f	1.84	0.68	···	···	···
Predicted θ	···	···	0°	37°	68°
Predicted h	···	···	1	2.73	4.17
Actual h	···	···	2	3	5

deposited, respectively. F_x is given by $F_x = (\sum_i m_i v_i^x v_i^x + \sum_{i \neq j} f_{ij}^x r_{ij}^x)/L_x$, where L_x is the simulation cell length in the X direction, m_i is the mass of atom i, and v_i^x, f_{ij}^x, and r_{ij}^x are the X component of the velocity of atom i, the force that atom j exerts on atom i, and the vector that separates atoms i and j, respectively. This force is the same across all possible cut surfaces perpendicular to the substrate surface. In the following, we report the biaxial mean value of this stress-thickness product $\sigma h = (\sigma_{xx} h + \sigma_{yy} h)/2$.

Figure 2 shows the calculated stress thickness versus number of adatoms. In order to minimize statistical noise, each data point represents the calculated stress thickness averaged over 40 measurements (following 10 ps MD relaxations). This figure shows that both the stress-thickness product and its derivative with respect to the number of adatoms (the stress in the newly added material) are negative. As the A-B bond strength increases (the A-B interface energy decreases), the magnitude of the compressive stress within the island increases. In other words, the island is under the largest compressive stress when the interface energy is smallest. These results are consistent with previous observations with Ag and Al islands on amorphous SiO_2 substrates [2].

To isolate the possible sources of measured compressive stress-thickness product, we rederive the Stoney equation, including the effects of surface or interface stresses. The effect of interface stress was considered by Ruud *et al.* [18] for the special case of continuous, multilayer films. Here we examine the case when the film is not yet continuous. Consider a cylindrical island with radius ρ and height t_f on a cylindrical substrate with radius R and thickness t_s. The total energy of the system can be written as $U_{\text{tot}} = U_{\text{bending}} + U_{\text{island}} + U_{\text{surface}}$, where subscripts refer to energy contributions from bending of the substrate, the island, and the surface or interface. The biaxial strain associated with pure bending is $\varepsilon = -\kappa z$, where κ denotes the curvature of the wafer and z is the distance from the neutral surface of bending ($\kappa > 0$ refers to the center of the wafer bent downward relative to the edges). The corresponding bending energy for the substrate is $U_{\text{bending}} = \pi R^2 E_s t_s^3 \kappa^2/[12(1-\upsilon)]$, where E_s, υ are the Young's modulus and Poisson ratio of the substrate, respectively [10]. The elastic energy stored within the island has contributions from both the residual stress (i.e., the mean stress in the absence of wafer curvature) and from substrate bending is $U_{\text{island}} = \pi \rho^2 t_f [\sigma_f - E_f \kappa (t_s + t_f)/2]^2 / E_f$, where E_f and σ_f are the Young's modulus of the island and mean stress inside the island. Since the surface or interface is biaxially strained, the energy associated with the surfaces or interfaces has contributions from the surface or interface energies themselves and the surface or interface stresses:

$$\begin{aligned} U_{\text{surface}} = {} & \pi\rho^2[\gamma_f - f_f(t_s + 2t_f)\kappa] + \pi\rho t_f(2\gamma_t - f_t t_s \kappa) \\ & + \pi\rho^2(\gamma_i - f_i t_s \kappa) + \pi(R^2 - \rho^2)(\gamma_s - f_s t_s \kappa) \\ & + \pi R^2(\gamma_s + f_s t_s \kappa), \end{aligned} \tag{1}$$

where γ_f, γ_t, γ_i, and γ_s (f_f, f_t, f_i, and f_s) are the surface energies (surface stresses) of the island upper surface, island side face, substrate/island interface, and substrate surface, respectively. Minimizing the system energy with respect to substrate curvature κ yields the relationship between substrate curvature, island stress, and surface or interface stresses (assuming a thick substrate $t_s \gg t_f$—this is valid for the simulations since the substrate is effectively semi-infinite, as described above):

$$\frac{E_s t_s^2}{6(1-\upsilon)} \kappa = \Theta \left[\sigma_f t_f + (f_f + f_i) + \frac{t_f}{\rho} f_t - f_s \right], \tag{2}$$

where the surface coverage (i.e., fraction of the substrate surface covered by the islands) is $\Theta = \pi\rho^2/\pi R^2$. Equation (2) is the surface stress-modified Stoney equation. This correction is important if the residual stress within the film is small (e.g., in homoepitaxy) or the film (island) is thin (small). [The corrected Stoney equation in Eq. (2) can be extended to the case of a continuous thin film on a substrate simply by letting t_f/ρ go to zero and Θ go to unity.]

If we assume the island is in mechanical equilibrium, the stress within the island is balanced by the surface or interface stresses: $\sigma_f t_f + f_f + f_i + (t_f/\rho) f_t = 0$ (this is a form of mechanical equilibrium). In this case, the surface stress-modified Stoney equation reduces to

$$\frac{E_s t_s^2}{6(1-\upsilon)} \kappa = -\Theta f_s. \tag{3}$$

This implies that the substrate curvature is a linear function of the substrate surface coverage with a slope given by minus the substrate surface stress, $-f_s$. Since the surface

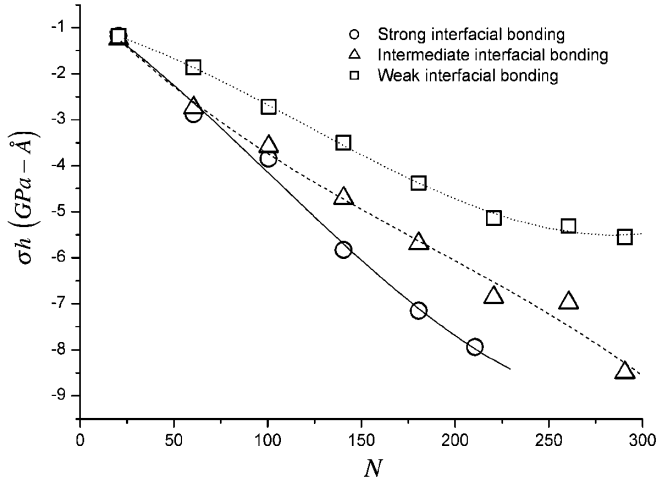

FIG. 2. Stress-thickness product as a function of the number of atoms deposited. Each data point represents an average of the data obtained during the deposition of 40 adatoms (to minimize statistical fluctuations).

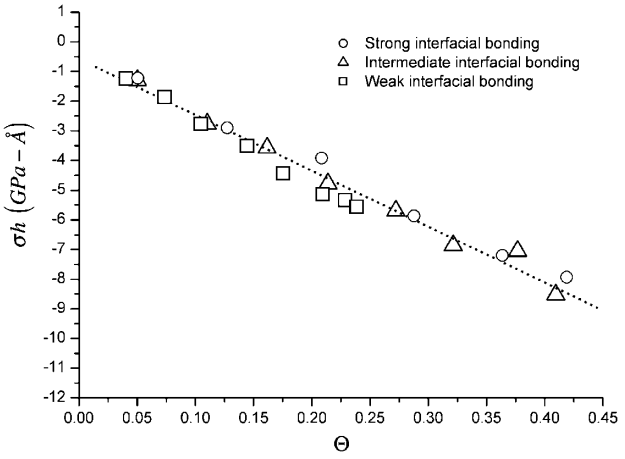

FIG. 3. Stress thickness vs substrate surface coverage Θ. The continuous curve is the best fit line. The slope of this line is -18.8 ± 0.9 GPa Å.

stress is most commonly found to be tensile, the substrate curvature measured during the island growth process will be negative with a magnitude that increases as growth proceeds. However, if the island is not in mechanical equilibrium or other sources of island stress (i.e., islands impingement, lattice mismatch) exist, Eq. (3) no longer holds and Eq. (2) should be applied.

We replot the stress-thickness data in Fig. 2 as a function of substrate surface coverage rather than number of atoms deposited. The result is shown in Fig. 3 for the three interfacial bond strength simulations reported above. The stress-thickness products for all three cases are a nearly linear function of surface coverage, and the σh data for all three interfacial bond strength simulation data sets collapse onto the same line with slope 18.8 ± 0.9 GPa Å. According to Eq. (3), this value should be equal to minus the surface stress of the substrate. The independent measure of the substrate surface stress reported in Table II is 18.4 GPa Å. The slope of the σh versus substrate surface coverage plot (Fig. 3) is in excellent agreement with the theoretical prediction that was based upon the assumption that the island is self-equilibrated (to within 2%). These observations show that the island itself is in mechanical equilibrium, and the compressive stress comes solely from the combined effects of surface or interface stresses together with substrate surface coverage. The measured stress-thickness product does not reflect the stress state inside the island itself. We can also explain why islands grown with a strong interface bond exhibit larger compressive stresses (as measured by the stress-thickness product): Given the same number of adatoms, islands grown with stronger interfacial bonding will have smaller wetting angles θ (and, therefore, exhibit larger compressive stress).

We have performed atomistic simulation of island growth and monitored stress and island morphology evolution as a function of numbers of adatoms deposited for islands with different island/substrate interface energies. The stress-thickness product was found to be compressive, in accordance with previous wafer curvature experiments. When the interface energy is small, the islands tend to be thin and broad and the magnitude of the compressive stress-thickness product is relatively large. To study the source of compressive stress, we rederive the Stoney equation, accounting for the effects of surface or interface stresses, and find that, in the limit that the island is self-equilibrated (the stress in the island balances the interface and surface stresses), the stress-thickness product is a linear function of the substrate coverage with slope equal to minus the substrate surface stress. This prediction is in excellent agreement with the simulation results. This shows that the island is in mechanical equilibrium and the stress-thickness product (wafer curvature) fails to represent the true stress state inside the island. The present simulations and theoretical analysis yield a simple, accurate, validated theory for stress development and demonstrate the limitation of wafer curvature experiments in obtaining film stress during the precoalescence stage of film growth.

We gratefully acknowledge the support of the U.S. Department of Energy, Grant No. DE-FG02-99ER45797.

[1] F. Spaepen, Acta Mater. **48**, 31 (2000).
[2] J. A. Floro, S. J. Hearne, J. A. Hunter, P. Kotula, E. Chason, S. C. Seel, and C. V. Thompson, J. Appl. Phys. **89**, 4886 (2001).
[3] G. G. Stoney, Proc. R. Soc. A **82**, 172 (1909).
[4] R. Abermann, R. Kramer, and J. Maser, Thin Solid Films **52**, 215 (1978).
[5] R. Abermann and R. Koch, Thin Solid Films **129**, 71 (1985).
[6] R. W. Hoffman, Thin Solid Films **34**, 185 (1976).
[7] W. D. Nix and B. M. Clemens, J. Mater. Res. **14**, 3467 (1999).
[8] E. Chason, B. W. Sheldon, L. B. Freund, J. A. Floro, and S. J. Hearne, Phys. Rev. Lett. **88**, 156103 (2002).
[9] R. C. Cammarata, T. M. Trimble, and D. J. Srolovitz, J. Mater. Res. **15**, 2468 (2000).
[10] S. P. A. Gill, H. Gao, V. Ramaswamy, and W. D. Nix, J. Appl. Mech. **69**, 425 (2002).
[11] C. Friesen and C. V. Thompson, Phys. Rev. Lett. **89**, 126103 (2002).
[12] C. Friesen, S. C. Seel, and C. V. Thompson, J. Appl. Phys. **95**, 1011 (2004).
[13] C. Friesen and C. V. Thompson, Phys. Rev. Lett. **93**, 056104 (2004).
[14] M. I. Baskes, Phys. Rev. Lett. **83**, 2592 (1999).
[15] M. I. Baskes, JOM **56**, 45 (2004).
[16] M. S. Daw and M. I. Baskes, Phys. Rev. Lett. **50**, 1285 (1983).
[17] To calculate the biaxial surface stress, we measure the energy of a perfect crystal and the same perfect crystal cleaved along the plane of interest. The slope of the difference between these energies as a function of biaxial strain is twice the biaxial surface stress.
[18] J. A. Ruud, A. Witvrouw, and F. Spaepen, J. Appl. Phys. **74**, 2517 (1993).